

The Mixed-metal Complex [Fe(bipe)(Au(CN)₂)₂MeOH] with Gold Clusters: A Novel Two-Dimensional Polycatenated Polyrotaxane Net Cliped by Auophilic Interaction

Haitao Xu, Gergely Juhász, Kazunari Yoshizawa*, Masashi Takahashi, Shinji Kanegawa and
Osamu Sato*

*Institute for Materials Chemistry and Engineering, Kyushu University,
6-1 Kasuga-koen, Kasuga, Fukuoka, 816-8580, Japan*

Institute for Materials Chemistry and Engineering, Kyushu University, Nishi-ku, Fukuoka 819-0395, Japan

Toho University, Department of Chemistry, 2-2-1 Miyama, Funabashi, Chiba 274-8510, Japan

E-mail: kazunari@ms.ifoc.kyushu-u.ac.jp and sato@cm.kyushu-u.ac.jp

Experimental section

All reagents and solvents used in the syntheses were of reagent grade and used without further purification. Elemental analyses of carbon, hydrogen, and nitrogen were conducted at the Center for Elemental Analysis, Kyushu University. Infrared spectroscopy studies were performed on a JASCO FT/IR-600 Plus spectrometer in the 4000–400 cm⁻¹ region. UV–Vis spectra were recorded on a Shimadzu UV-3100PC spectrometer with an MPC 3100 unit.

Magnetic susceptibility measurements were carried out on a Quantum Design MPMS-5S SQUID system. Experimental susceptibilities were corrected for diamagnetism of the background the sample holder and its constituent atoms.

X-ray diffraction experiment was carried out on a Rigaku CCD diffractometer using Mo-K α radiation ($\lambda = 0.71073 \text{ \AA}$) at 123(2) K. The following software was used for data collection, cell refinement and data reduction: CrystalClear 1.3.5 (Rigaku) and RAPID AUTO 2.01 (Rigaku). The structures were solved and refined using the direct method and full-matrix method based on F^2 using the SHELXL97 software package (Sheldrick, 1997). All non-hydrogen atoms were refined anisotropically and their positions were generated geometrically.

¹⁹⁷Au Mössbauer spectra were measured at 20 K as described previously.¹ The ¹⁹⁷Pt/Pt Mössbauer source was prepared by neutron irradiation of a 100 mg disc of enriched metallic ¹⁹⁶Pt in the JRR-4 reactor of JAERI. The Mössbauer spectra were measured at Toho University using a Mössbauer spectrometer from Wissel (MDU-1200 function generator, DFG-1200 driving unit, MVT-100 velocity transducer and MVC-1200 laser calibrator). The isomer shift is given relative to the ¹⁹⁷Pt/Pt source at 20 K.

1) M. Takeda, M. Takahashi, Y. Ito, T. Takano, M. A. Bennett, S. K. Bhargava, *Chem. Lett.* 1990, 543

Table 1 Crystallographic data for the complex [Fe(bipe)(Au(CN)₂)₂MeOH].

Empirical formula	C ₁₇ H ₁₅ Au ₂ FeN ₆ O
Formula weight	769.13
Space group	P -I (no. 2)
T (K)	123(2)
a (Å)	7.227(3)
b(Å)	10.992(4)
c(Å)	13.404(6)
α ^o	79.21(2)
β ^o	79.17(2)
γ ^o	74.06(2)
V (Å ³)	995.21(70)
Z	2
ρ _{cal.} Mg/m ³	2.566
R	0.0250
Rw	0.0634
GOF	1.100

Table 2. Selected bond lengths (Å) of the complex [Fe(bipe)(Au(CN)₂)₂MeOH]

N6—C15	1.333(17)	Au2—C2	1.986(21)
C8—C7	1.402(9)	C5—O1	1.426(17)
N6—C16	1.343(13)	Au2—C2 ⁱⁱⁱ	1.986(21)
C8—C11	1.507(19)	Au3—C3 ^{iv}	1.980(25)
N6—Fe4 ⁱ	2.210(13)	Au3—C3	1.980(25)
C6—N5	1.336(10)	Au3—Au1 ^v	3.103(40)
C16—C17	1.379(11)	C4—N4	1.130(11)
C6—C7	1.371(18)	Au3—Au1 ^{vi}	3.103(40)
C14—C15	1.389(11)	Fe4—O1	2.118(25)
C14—C13	1.388(13)	C3—N3	1.154(16)
C2—N2	1.142(14)	Fe4—N3	2.152(28)
C12—C11	1.524(18)	C9—C10	1.388(18)
C13—C17	1.400(18)	Fe4—N2	2.152(27)
C13—C12	1.499(11)	C9—C8	1.39(1)
Au1—C1	1.991(16)	Fe4—N1	2.184(13)
Au1—C4	2.001(15)	Fe4—N5	2.200(27)
Au1—Au3 ⁱⁱ	3.103(40)	C10—N5	1.356(8)
C1—N1	1.139(11)	Fe4—N6 ^j	2.210(13)

Table 3. Selected bond Angles (°) of the complex [Fe(bipe)(Au(CN)₂)₂MeOH]

C15—N6—C16	116.46(41)	N3—Fe4—N1	87.75(16)
C15—N6—Fe4 ⁱ	119.71(34)	C10—C9—C8	120.57(40)
C16—N6—Fe4 ⁱ	123.82(34)	N2—Fe4—N1	88.24(16)
N6—C16—C17	123.71(49)	O1—Fe4—N5	177.93(13)
C8—C11—C12	114.22(40)	N3—Fe4—N5	88.75(15)
C15—C14—C13	121.39(44)	N5—C10—C9	122.77(47)
N6—C15—C14	122.93(46)	N2—Fe4—N5	91.39(15)
C16—C17—C13	120.58(49)	N1—Fe4—N5	91.36(15)
C14—C13—C17	114.88(41)	O1—Fe4—N6 ⁱ	89.03(14)
C14—C13—C12	124.22(42)	C9—C8—C7	115.82(40)
N1—C1—Au1	174.56(46)	N3—Fe4—N6 ⁱ	91.83(15)
C17—C13—C12	120.89(45)	C9—C8—C11	122.93(38)
C1—Au1—C4	175.90(21)	N2—Fe4—N6 ⁱ	92.18(15)
C1—Au1—Au3 ⁱⁱ	87.78(13)	C7—C8—C11	121.25(41)
C4—Au1—Au3 ⁱⁱ	95.91(15)	N1—Fe4—N6 ⁱ	179.12(16)
C2—Au2—C2 ⁱⁱⁱ	180.00(19)	N5—C6—C7	123.92(46)
C3 ^{iv} —Au3—C3	179.99(19)	N5—Fe4—N6 ⁱ	89.41(15)
C3 ^{iv} —Au3—Au1 ^v	86.51(13)	C3—N3—Fe4	175.40(38)
N4—C4—Au1	177.71(49)	C6—N5—C10	116.48(43)
C3—Au3—Au1 ^v	93.49(13)	C6—C7—C8	120.43(46)
O1—Fe4—N3	89.94(14)	C6—N5—Fe4	121.60(33)
C3 ^{iv} —Au3—Au1 ^{vi}	93.49(13)	C10—N5—Fe4	121.82(33)
O1—Fe4—N2	90.03(13)	C2—N2—Fe4	169.42(38)
C3—Au3—Au1 ^{vi}	86.51(13)	N2—C2—Au2	176.49(40)
N3—Fe4—N2	175.99(16)	C1—N1—Fe4	161.00(42)
Au1 ^v —Au3—Au1 ^{vi}	180.00(2)	C13—C12—C11	116.51(41)
O1—Fe4—N1	90.19(14)	C5—O1—Fe4	125.27(27)
N3—C3—Au3	178.95(40)		

Symmetry codes:

(i) 1-x, 1-y, 1-z; (ii) 1+x, y, z; (iii) 3-x, 1-y, 1-z; (iv) 1-x, 2-y, -z; (v) -1+x, y, z; (vi) 2-x, 2-y, -z.

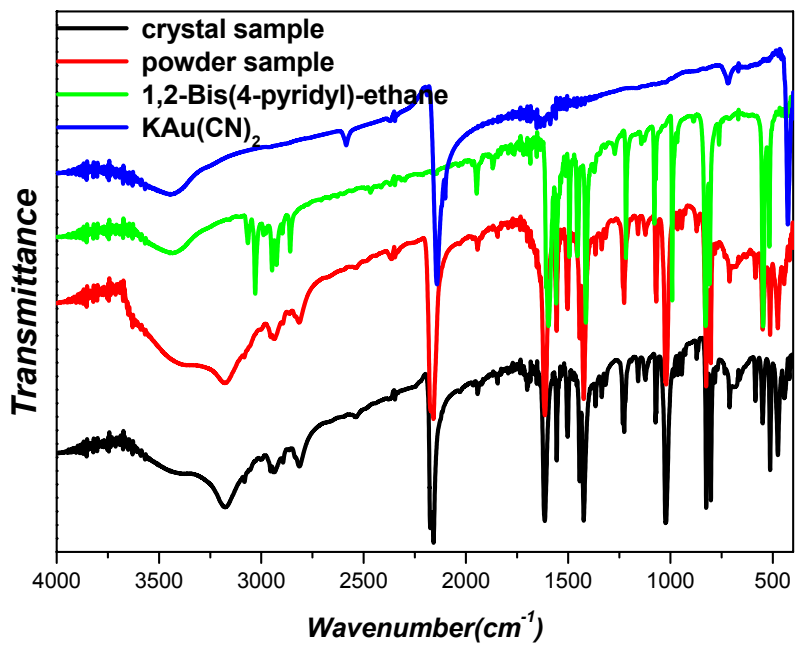


Figure S1. Infrared spectroscopy of the complex $\text{Fe}(\text{bipe})(\text{Au}(\text{CN})_2)_2\text{MeOH}$ at the room temperature.

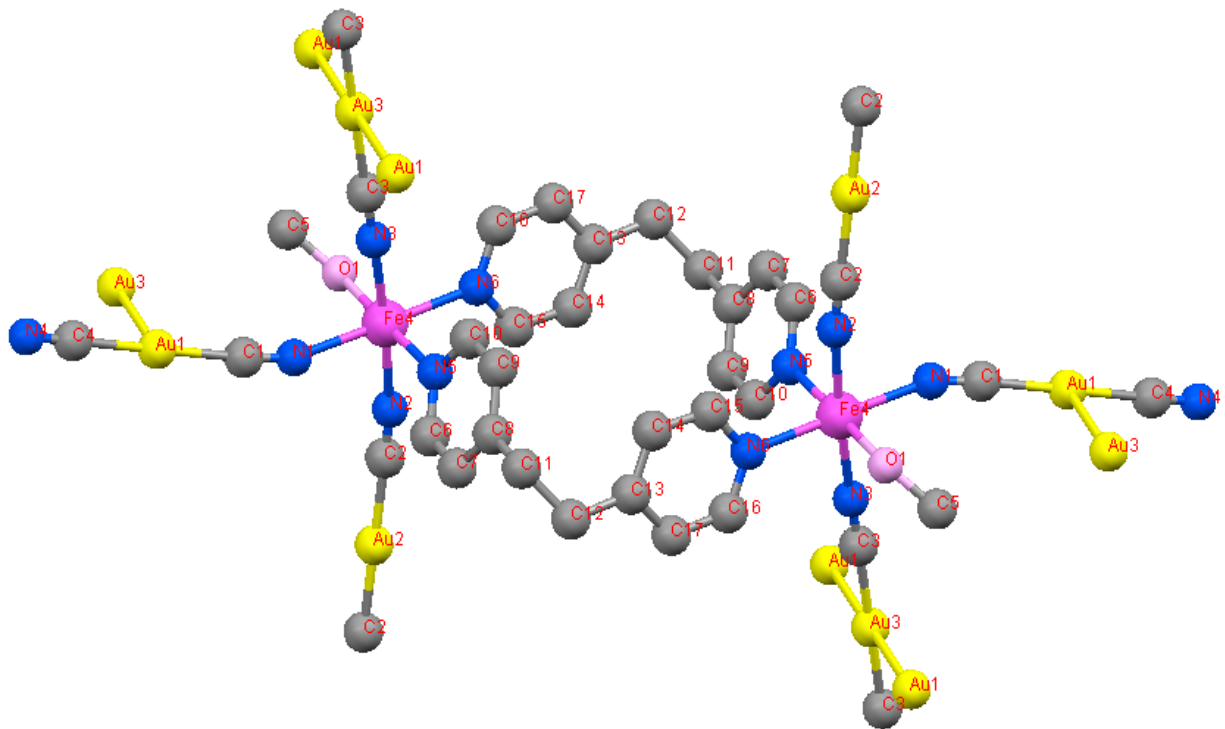


Figure S2. The ORTEP plot of the structure in the crystal $[\text{Fe}(\text{bipe})(\text{Au}(\text{CN})_2)_2\text{MeOH}]$

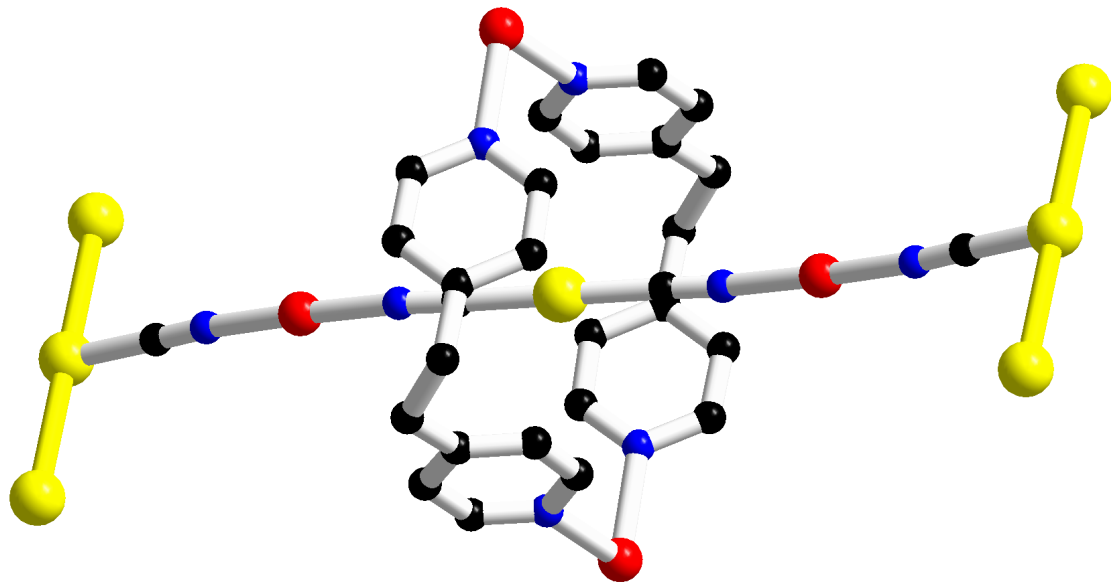


Figure S3. Mixed-metal rod Fe-Au passing through the metal-ring $\text{Fe}_2(\text{bipe})_2$ in the crystal $[\text{Fe}(\text{bipe})(\text{Au}(\text{CN})_2)_2\text{MeOH}]$

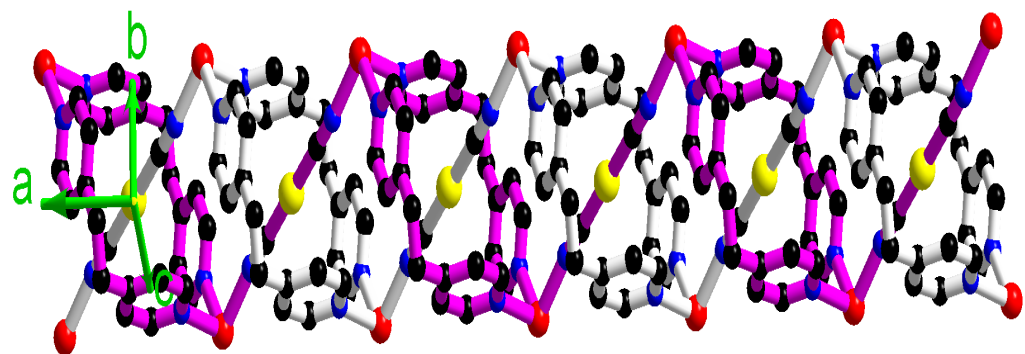


Figure S4. Polyrotaxane column present in the $[\text{Fe}(\text{bipe})(\text{Au}(\text{CN})_2)_2\text{MeOH}]$ framework. The components of two independent networks are indicated by purple and white connections respectively. (Hydrogens and MeOH are omitted for clarity)

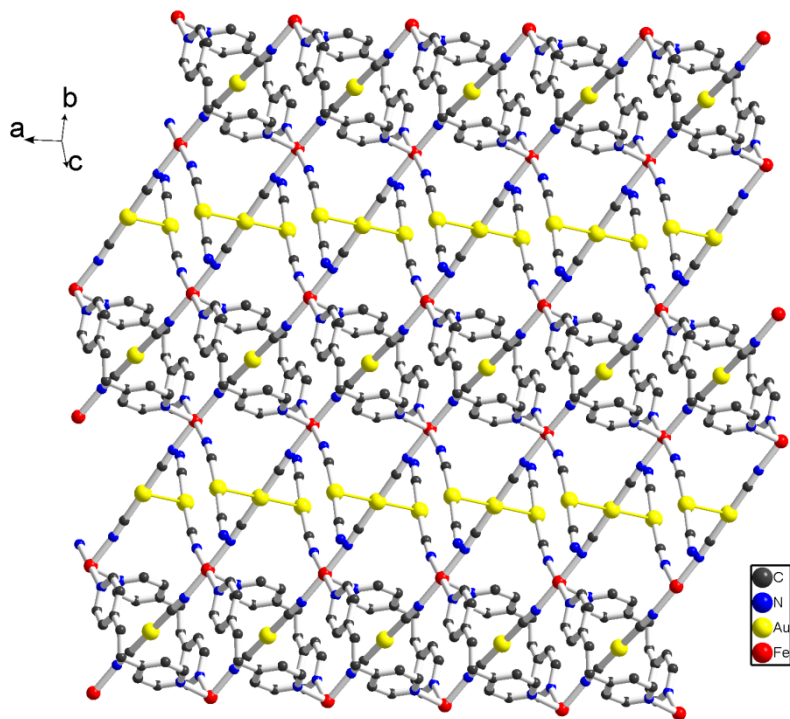


Figure S5. 2D-layer structural diagram of the crystal $[Fe(bipe)(Au(CN)_2)_2MeOH]$ with gold clusters (MeOH is omitted for clarity)

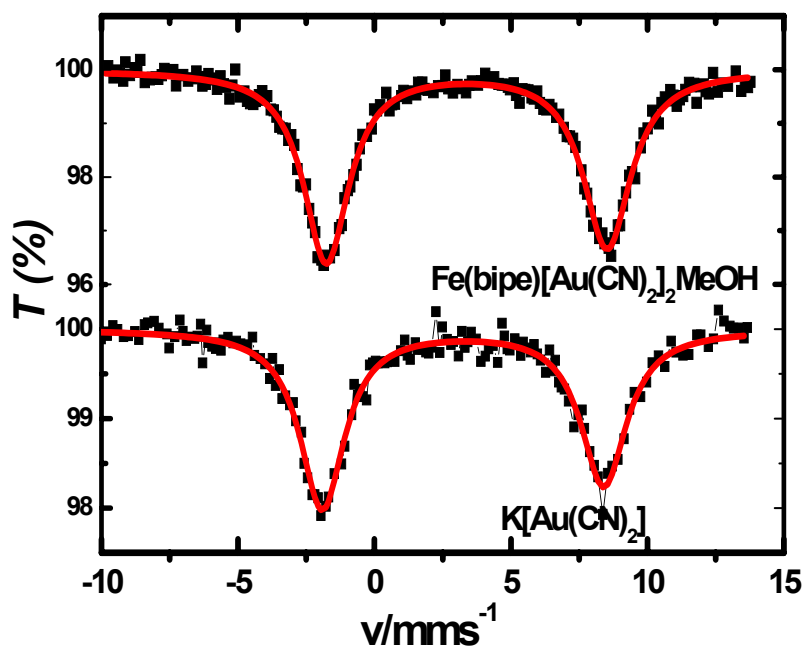


Figure S6. ^{197}Au Mössbauer spectrum of $[\text{Fe}(\text{bipe})(\text{Au}(\text{CN})_2)_2\text{MeOH}]$ and $\text{K}[\text{Au}(\text{CN})_2]$ at 20 K

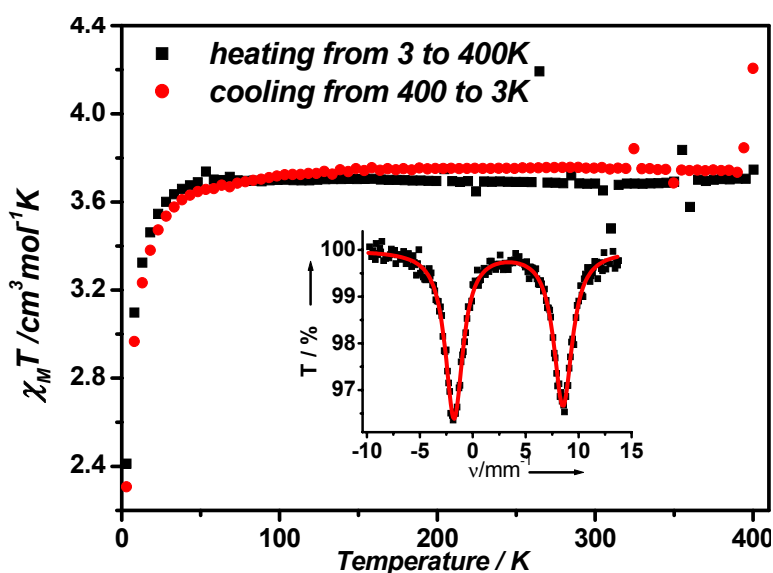


Figure S7. Temperature dependence of $\chi_m T$ - T plots of the powder sample of the complex $[\text{Fe}(\text{bipe})(\text{Au}(\text{CN})_2)_2\text{MeOH}]$. Inset : ^{197}Au Mössbauer spectrum of the complex $[\text{Fe}(\text{bipe})(\text{Au}(\text{CN})_2)_2\text{MeOH}]$ at 20 K

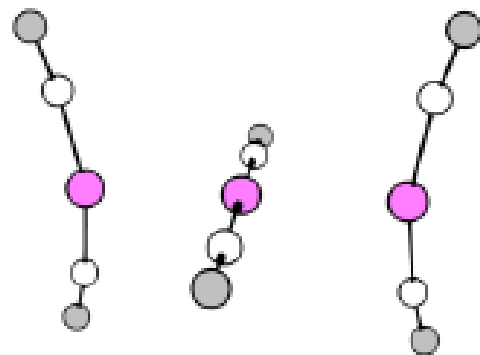


Figure S8. The structure of $[Au(CN)_2]^{3+}$ in the complex $Fe(bipe)(Au(CN)_2)_2MeOH$.

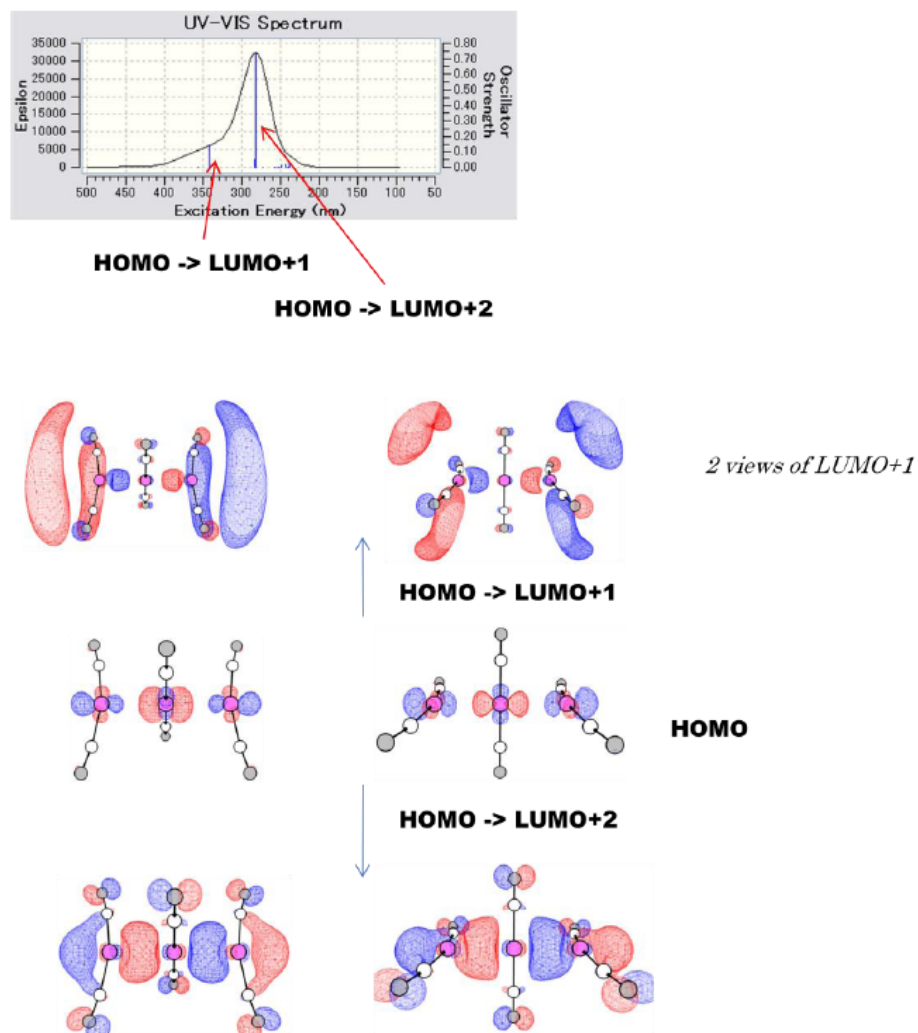


Figure S9. The UV-Vis active transitions of $[Au(CN)_2]^{3+}$ from HOMO ($d\sigma^*\sigma^*$) to LUMO+1 ($p\sigma\sigma$) and to LUMO +2 ($p\sigma\sigma$)

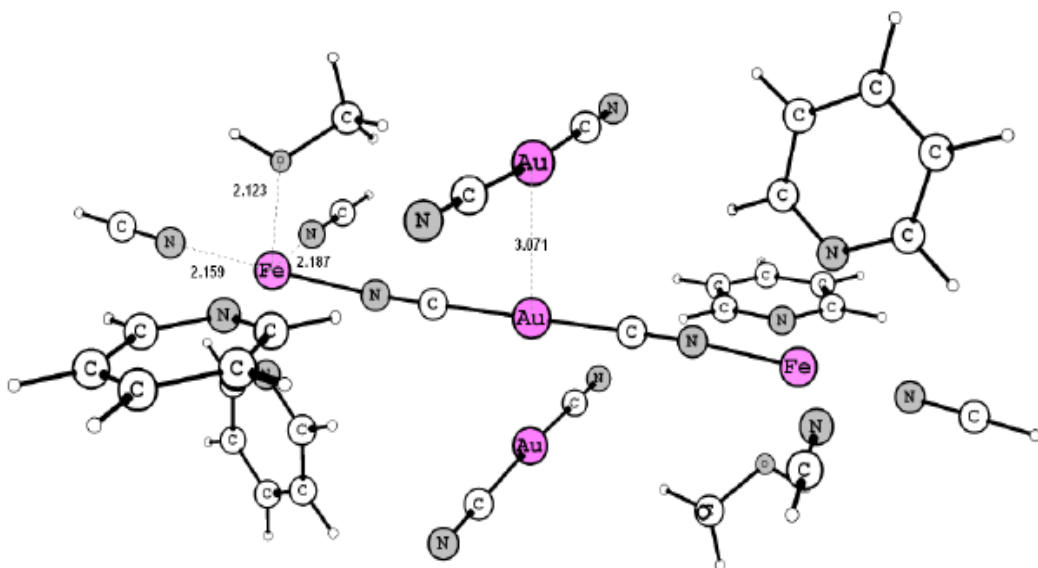


Figure S10. The Structure of $[Fe(II)(py)_2MeOH](CNH)_2]_2[Au(CN)_2]_3$

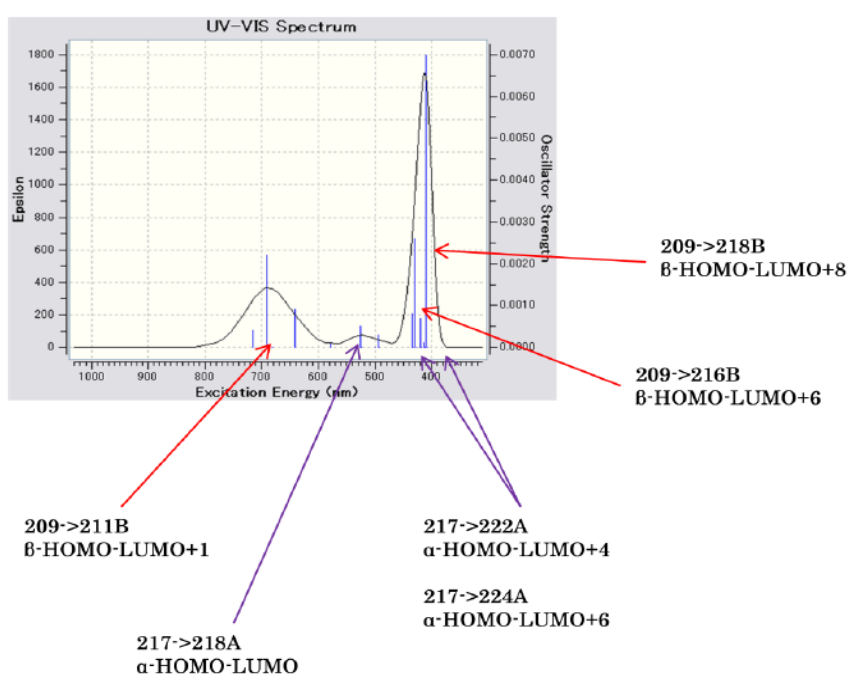


Figure S11. Predicted UV-Vis spectrum (from first 30 transition) of $Fe(II)(py)_2MeOH](CNH)_2]_2[Au-(CN)_2]_3$

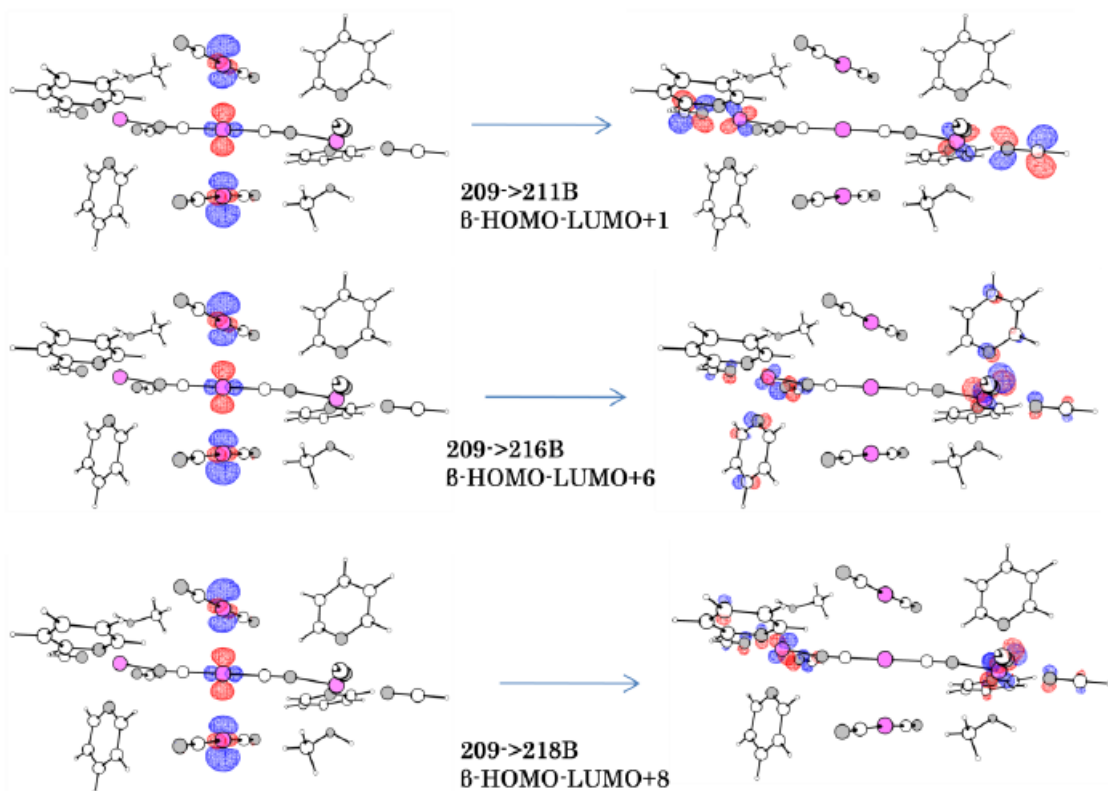


Figure S12. The UV-Vis active transition between spin-down orbitals (β) from HOMO ($d_{Au}\sigma^*\sigma^*$) to ($d_{Fe-L}\pi^*$) orbitals

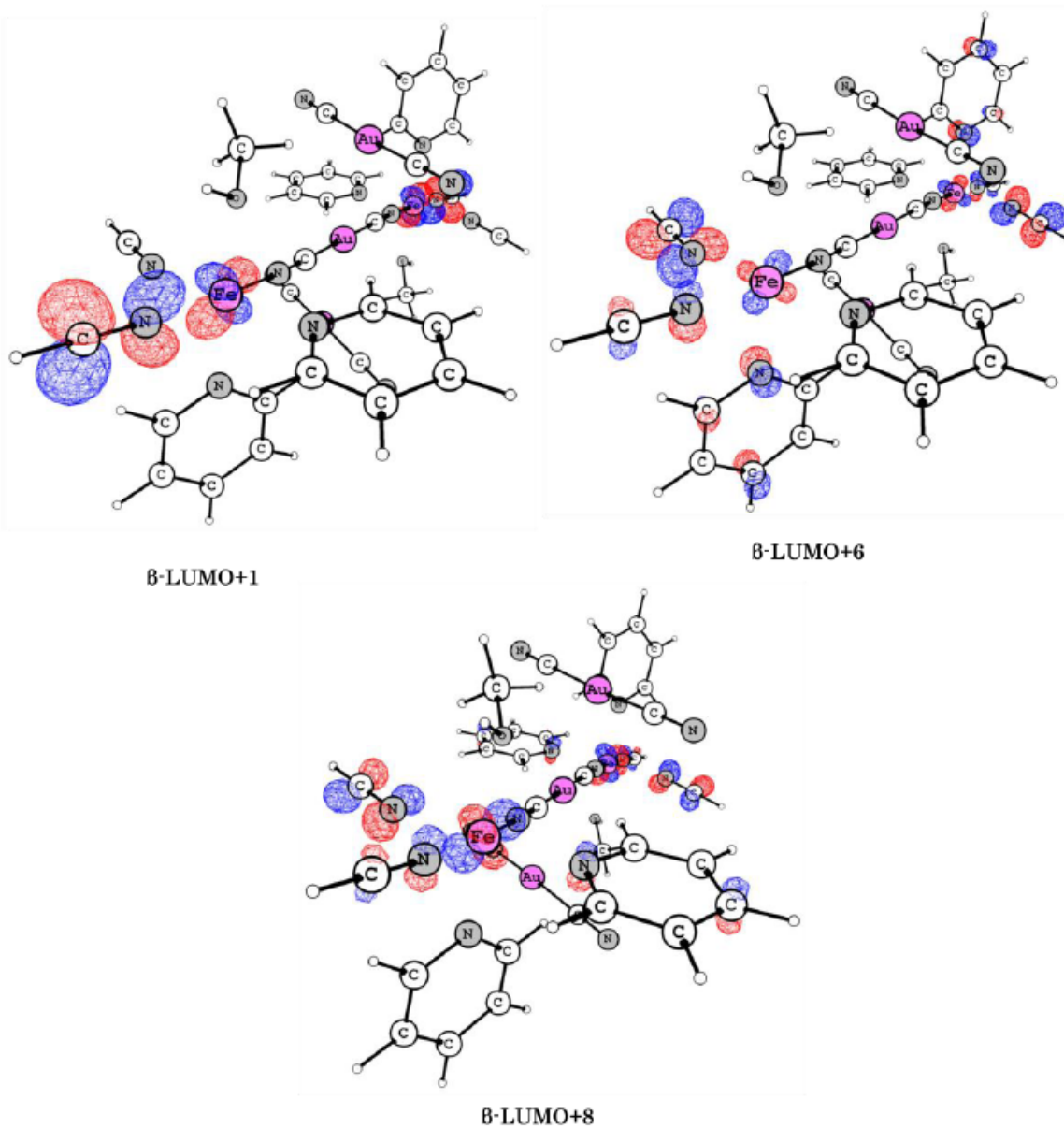


Figure S13. The UV-Vis active transition between spin-down orbitals (β): ($d_{Fe-L}\pi^*$) orbitals (zoomed up)

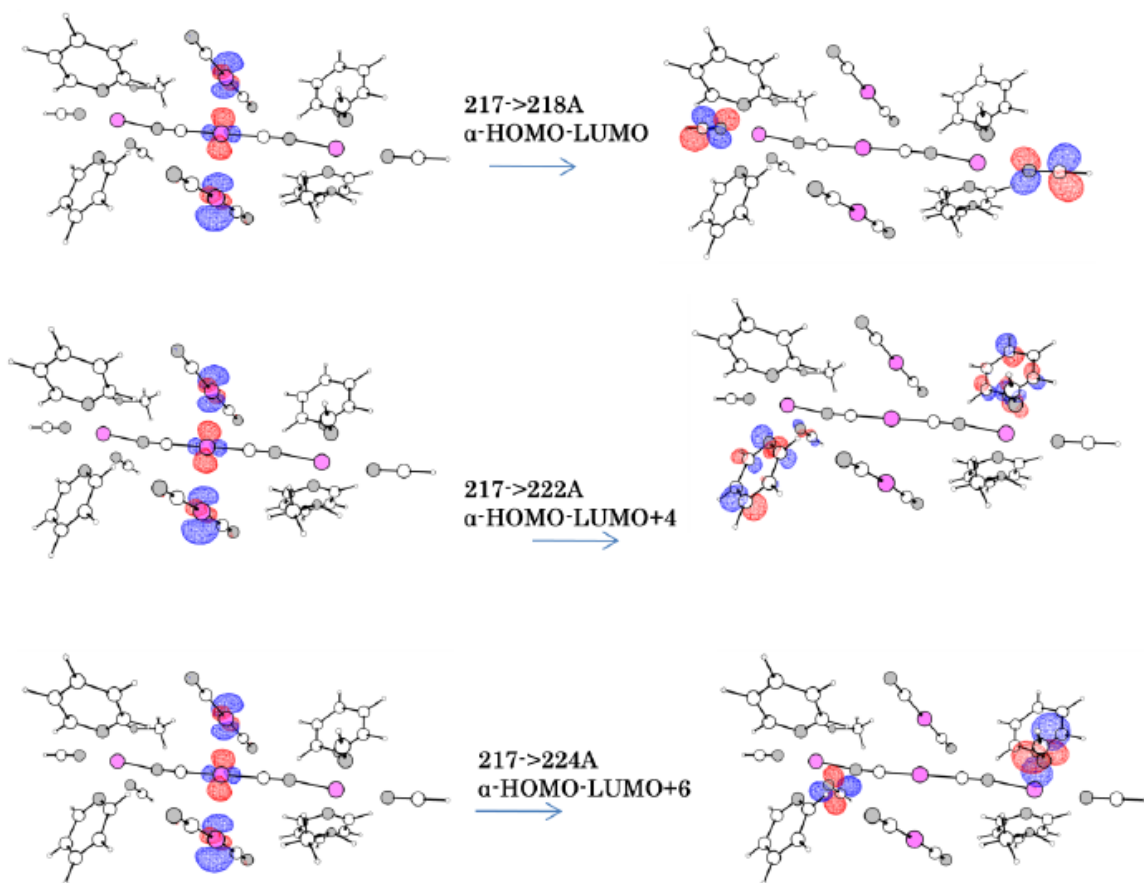


Figure S14. The UV-Vis active transition between spin-up orbitals (α) from α -HOMO ($d_{Au}\sigma^*\sigma^*$) to ($p_L\pi^*$) orbitals

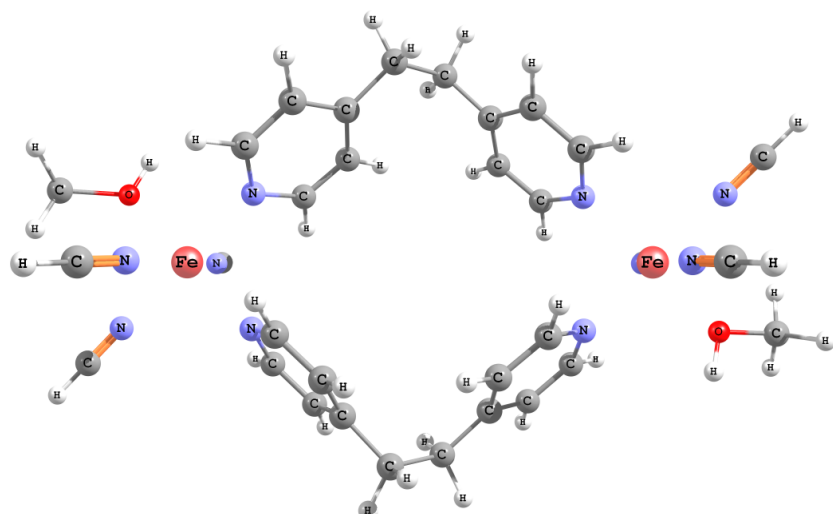


Figure S15. The structure of an empty $Fe_2(bipe)_2$ -type macrocycle $[Au(CN)_2]_3^{3+}$

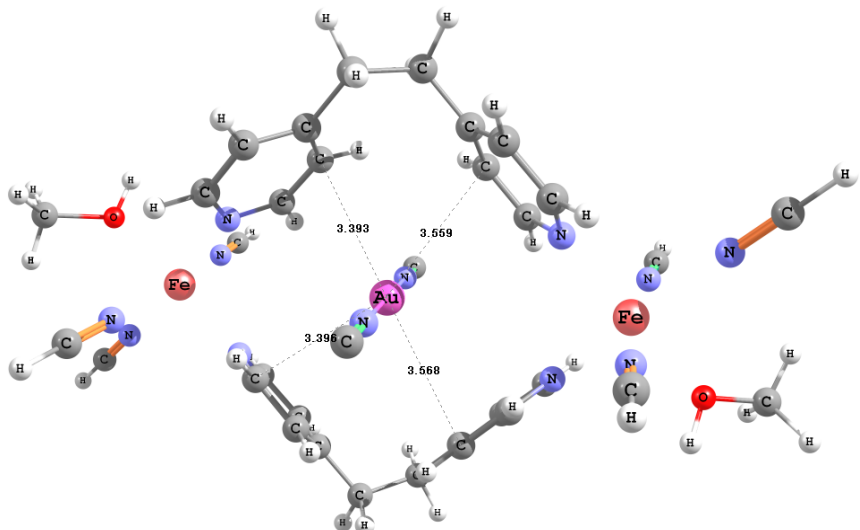
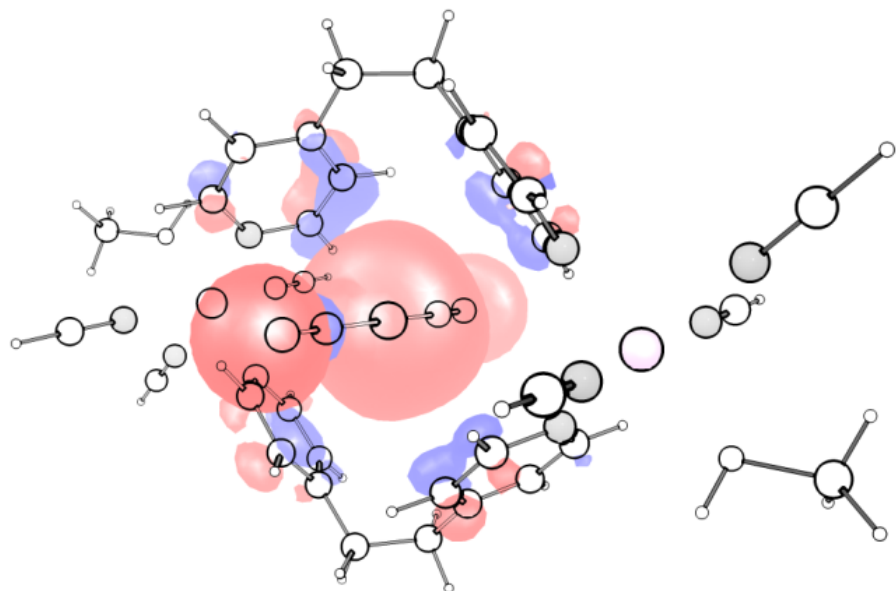


Figure S16. The structure of an $Fe_2(bipe)_2$ -type macrocycle with $[Au(CN)_2]_3^{3+}$ axle with short contacts

α HOMO



α HOMO-7

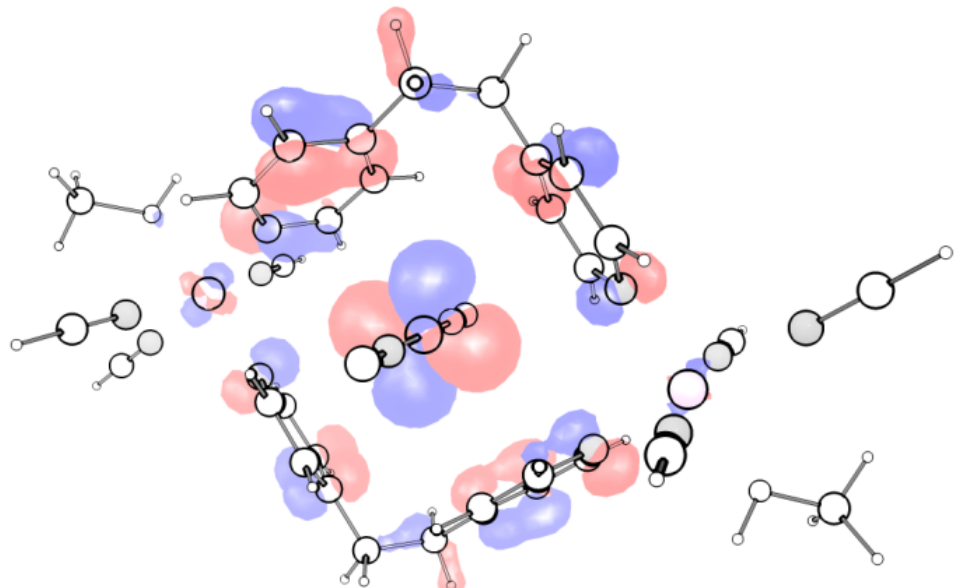


Figure S17. Examples for orbital interaction between the macrocycle and the axle in the $Fe_2(bipe)_2$ -type macrocycle with $[Au(CN)_2]^{3+}$ axle: α HOMO (up) and α HOMO-7 (down)